A Hybrid Level Set Segmentation for Medical Imagery

Seongjai Kim, *Member, IEEE,* and Hyeona Lim

***Abstract*— This article is concerned with a level set segmentation (active contour) algorithm for medical imagery. Due to difficulties such as noise and unclear edges, it is often challenging to obtain a reliable segmentation for medical images. In addition to introducing a new hybrid model which combines a gradient-based model and the Mumford-Shah (gradient-free) method, we study the so-called method of background subtraction (MBS) in order to improve reliability of the new model. A linearized alternating direction implicit method is applied for an efficient time integration. For a fast convergence, we also suggest effective initialization strategies for the level set function. The resulting algorithm has proved to locate the desired edges in 2-4 iterations.**

I. Introduction

The major objective in image segmentation is to identify an image as a collection of parts, each of which has a strong correlation with real-world objects. Parts in an image can be separated by a contour. Thus, the practical goal of image segmentation is to divide the image into parts by inserting contours.

Segmentation methods of considerable interest in engineering applications are the zero crossing [5], [9], thresholding [1], [8], region-based segmentation [10], [19], and watershed [2], [11], [12], [13], [16]. Recently, level set-based segmentation methods are introduced in image segmentation [3], [4], [17], [20].

The idea of the level set methods is as follows: For a given image u^0, we denote the desired contours of edges by Γ. When a level set function $\phi : \Omega \to \mathbb{R}$ [18] is incorporated with a segmentation method, the contours of edges are identified by the zero-level set, i.e., $\Gamma = \{\mathbf{x} : \phi(\mathbf{x}) = 0\}$. Changes in values of the level set function can reform the contours of the desired edges. Such mathematical techniques are called the methods of *active contours* or *snakes*. Effectiveness and efficiency of the snake methods depend strongly on a complementary function (CF), which we define in this article as a function that invokes a driving force for the level set function ϕ. The CF must be incorporated in such a way that it is easy to compute and introduces a reliable driving force for the change of the level set function and therefore the zero-level set.

For the last decade or so, gradient methods such as watershed algorithms [12], [13], [16] and PDE-based active contour models (or snakes) [14], [20] have been actively developed for image segmentation. These gradient-based methods utilize the so-called *gradient maps* to either locate edges directly or provide driving forces in order for the contours to march toward the desired locations. However, these methods have proved erroneous when in particular the image is noisy or its edges are not clear. As a result, the segmentation procedure requires a series of post-processing steps that are often cumbersome and model-based.

To overcome such difficulties, Chan and Vese [3], [4] have studied a level set formulation of the Mumford-Shah segmentation [17], called the *Mumford-Shah-Chan-Vese* (MSCV) model, which does not have to utilize the gradient information of the original image u^0 for the stopping process. Instead, the stopping term is based on the minimization of a certain energy functional measured from the difference between the original image and a pair of locally smooth cartoon images. In this article, we call the cartoon images the *complementary functions* (CFs) of u^0. The CFs must be updated appropriately, during the computation, to provide the level set function with a reliable driving force. The MSCV model can detect edges both with and without gradients, e.g., objects that are smooth or even have discontinuous boundaries. Furthermore, the model can detect interior boundaries automatically. However, the MSCV model exhibits a fundamental drawback unless the original image u^0 is essentially binary and has yet to be improved for general images.

In this article, we develop a level set segmentation algorithm which hybridizes gradient-based methods and the MSCV (gradient-free) method, for an efficient and reliable segmentation.

An outline of the article is as follows. In Section II, we introduce a new hybrid model and the method of background subtraction (MBS) to improve the reliability of the model. We introduce new initialization techniques in Section III for a faster convergence. Finally in Section IV, we present some numerical results of the new model, comparing with those of the MSCV model. The last section includes conclusions.

II. New Methods

In this section, we begin with a new hybrid model, which combines a gradient-based model by Zhao *et al.* (ZCMO) [20] and a gradient-free model by Mumford-Shah-Chan-Vese (MSCV) [3], [4], [17]. Then, in order to improve reliability for the model, we consider and refine the so-called method of

SK: Department of Mathematics and Statistics, Mississippi State University, Mississippi State, MS 39762-5921 USA Email: skim@math.msstate.edu. The work of this author is supported in part by NSF grant DMS-0312223.

HL: Department of Mathematics and Statistics, Mississippi State University, Mississippi State, MS 39762-5921 US Email: hlim@math.msstate.edu

background subtraction (MBS), which was first introduced by Kim [15].

A. A new hybrid model

We first note that the curvature term in the MSCV model has the major role of smoothing the level set function, which can be replaced by a reasonable smoothing term, e.g., the corresponding term in the ZCMO model. We explicitly define the hybrid model: for some $\alpha,\ \beta \geq 0$,

$$\begin{aligned} \frac{\partial \phi}{\partial t} - \alpha\,|\nabla\phi|\,\nabla\cdot\Big(g\frac{\nabla\phi}{|\nabla\phi|}\Big) \\ = \beta\,(u^+ - u^-)\Big(u^0 - \frac{u^+ + u^-}{2}\Big), \end{aligned} \tag{1}$$

where g is defined as, for some $\zeta > 0$ and $p \geq 1$,

$$g(\nabla u^0) = \frac{1}{\zeta + |J * \nabla u^0|^p}. \tag{2}$$

Here u^0 is the given image, $u^\pm$ are CFs, and J denotes a Gaussian of variance σ^2.

One may select $u^\pm$ as the solution of the elliptic equations as in the MSCV model. However, due to some drawbacks of the model, new CFs must be found in order to incorporate local gradient information more effectively into the level set iteration; see Kim [15] for a set of effective CFs.

We note that the level set function in the (gradient-based) ZCMO model [20] evolves depending on *local* properties of the edge detector $g = g(\nabla u^0)$. Thus one should initialize the level set function accurately for the model to detect the desired boundaries satisfactorily. It is also known that the model can hardly find interior boundaries or contours that are very smooth or have discontinuous boundaries. Therefore, our hybrid model (1) can be viewed as a variant of the ZCMO model, incorporating the forcing term in the right side in order to minimize such drawbacks. For an efficient computation of (1), one can employ an incomplete (linearized) backward Euler time-stepping procedure and the *alternating direction implicit* (ADI) perturbation [6], [7].

B. The method of background subtraction (MBS)

Consider a synthetic image which includes objects on an oscillatory background, as shown in Figure 1(top). When the MSCV model is applied for the image, it easily produces extra boundaries as in Figure 1(bottom). Such extra boundaries have been observed from various experiments; the model assumes some smooth portions as parts of boundaries. This property of the MSCV model is not independent from the claim in [3], [4]: *the method can detect smooth boundaries*. The ability of detecting smooth boundaries is not always advantageous for the segmentation of general images, shown in this example. In order to overcome this difficulty, Kim [15] has introduced the so-called *method of background subtraction* (MBS) for more efficient segmentation of images with general backgrounds. Here we refine the MBS.

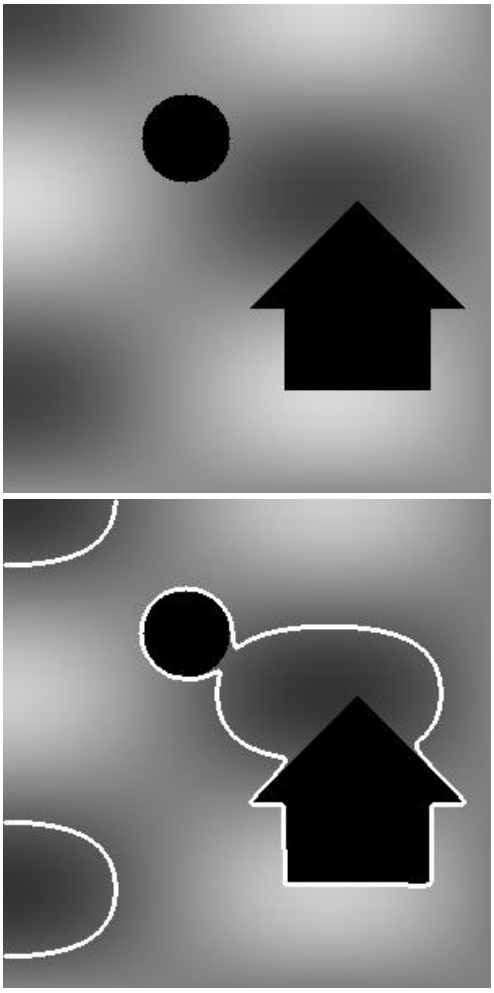

Fig. 1. Segmentation for a synthetic image: (top) the original image and (bottom) the segmentation with the MSCV model.

Let the image u^0 be decomposed as

$$u^0 = \widetilde{u} + \delta u, \quad \widetilde{u} \leq u^0, \tag{3}$$

where $\widetilde{u}$ is a smooth component (the background) of the image. Then, the segmentation is applied to δu.

For an illustration of the MBS, see Figure 2. There the background ($\widetilde{u}$) and the edge-component (δu) are depicted schematically for a given synthetic image u^0. As one can see from the figure, segmentation algorithms can detect the boundaries of δu more effectively than those of u^0, provided that the background is smooth enough not to distract the edges. Note that the edge-component δu may become an *essentially binary* image, for which the segmentation is much easier. Here the problem is *how to compute an effective background*.

In the following, we suggest a strategy for computing a smooth background, which has been motivated from the multi-grid (multi-resolution) methods:

(i) *Select a coarse mesh* $\{\Omega_{ij}\}$ *for the image domain* Ω. Each element Ω_{ij} in the coarse mesh contains $m_x \times m_y$ pixels of the image u^0, for some $m_x,\ m_y \geq 1$.

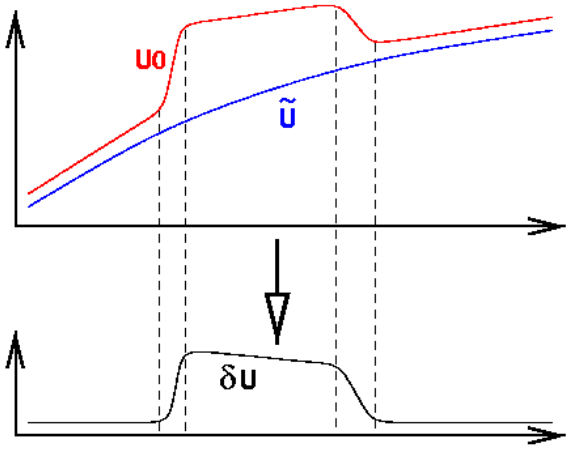

Fig. 2. A schematic illustration of the method of background subtraction.

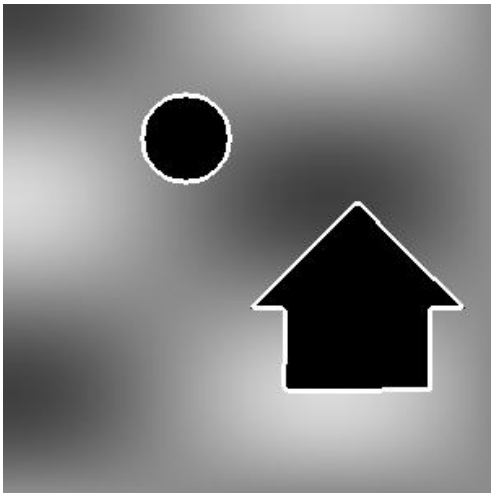

Fig. 3. The segmentation of synthetic data by the new model.

(ii) *Choose a coarse image* u_c *on* $\{\Omega_{ij}\}$: for example,

$$u_{c,ij} \;=\; (a_{ij} + m_{ij})/2,$$

where $u_{c,ij}$ denotes the value of u_c on Ω_{ij} and

$$\begin{array}{rcl} a_{ij} & = & \text{the arithmetic average of } u^0 \text{ on } \Omega_{ij}, \\ m_{ij} & = & \text{the minimum on } \Omega_{ij}. \end{array}$$

(iii) *Smooth* u_c, *with* $u_c^{\text{new}} \le u_c^{\text{old}}$ *pointwisely*. For example, apply a few iterations of the *four-point averaging* in a modified form:

$$\begin{array}{rcl} u_{c,ij}^{k+1/2} & = & \dfrac{u_{c,i-1,j}^k + u_{c,i+1,j}^k + u_{c,i,j-1}^k + u_{c,i,j+1}^k}{4}, \\ u_{c,ij}^{k+1} & = & \min(u_{ij}^0,\, u_{c,ij}^{k+1/2}). \end{array} \tag{4}$$

(iv) *Prolongate* u_c *to the original mesh* Ω, *for* u_f. One may apply simply the bilinear interpolation for the prolongation.

(v) *Smooth the prolongated image* u_f. Apply a few iterations of a standard local averaging algorithm.

(vi) *Assign the result for* $\widetilde{u}$.

In the above algorithm for the computation of $\widetilde{u}$, one should determine parameters: the element size of the coarse mesh (m_x and m_y) and the iteration numbers for the smoothing algorithms. It is apparent that the number of smoothing iterations depends on the element size of the coarse mesh. In this paper, we will select the parameters experimentally. It has been numerically verified that the resulting segmentation is *weakly* sensitive to the parameters; the most sensitive parameters are m_x and m_y which determine the size of coarse mesh.

Remark: When the segment algorithm must detect a darker object, then the decomposition (3) can be performed with $\widetilde{u} \ge u^0$, for which the corresponding solution in the coarse mesh can be computed by (4) with "min" replaced by "max".

III. Initialization Techniques

For a faster convergence in detecting edges, one may consider accurate and appropriate initialization of the level set function. In this section, we will present a strategy for an effective initialization.

A. Initialization of the level set function

The given image u^0 can be utilized for an accurate initialization of ϕ (in fact, the zero level set of ϕ). We initialize the value of ϕ^0 as follows:

$$\phi^0 \;=\; u^0 \;-\; \overline{u^0} \tag{5}$$

where $\overline{u^0}$ is the ℓ^2-average of u^0.

Note that for simple binary images, the above initialization is already locating the desired edges quite accurately. For more general images, we would better apply the MBS to get $\delta u = u^0 - \widetilde{u}$. Then, we can initialize ϕ as in (5), replacing u^0 by δu.

B. Modification of the initialization

For a prompt response of the level set function to the driving force during the iteration, it is natural to restrict the values of ϕ^0 (the initialization of ϕ) to be near zero, by scaling or by imposing upper and lower limits. For example, when $\phi_{\max} > 0$ denotes the desired maximum value, the initial values of the level set function can be adjusted as

$$\phi_{ij}^0 \;\leftarrow\; \phi_{\max} \cdot \frac{2}{\pi} \tan^{-1}(\phi_{ij}^0). \tag{6}$$

Note that the right side is a smooth, symmetric, and increasing function, having the values in $(-\phi_{\max}, \phi_{\max})$. Let $u^0 \in [0,1]$ (by scaling by 1/255). Then one may set $\phi_{\max} \sim 10^{-4}$.

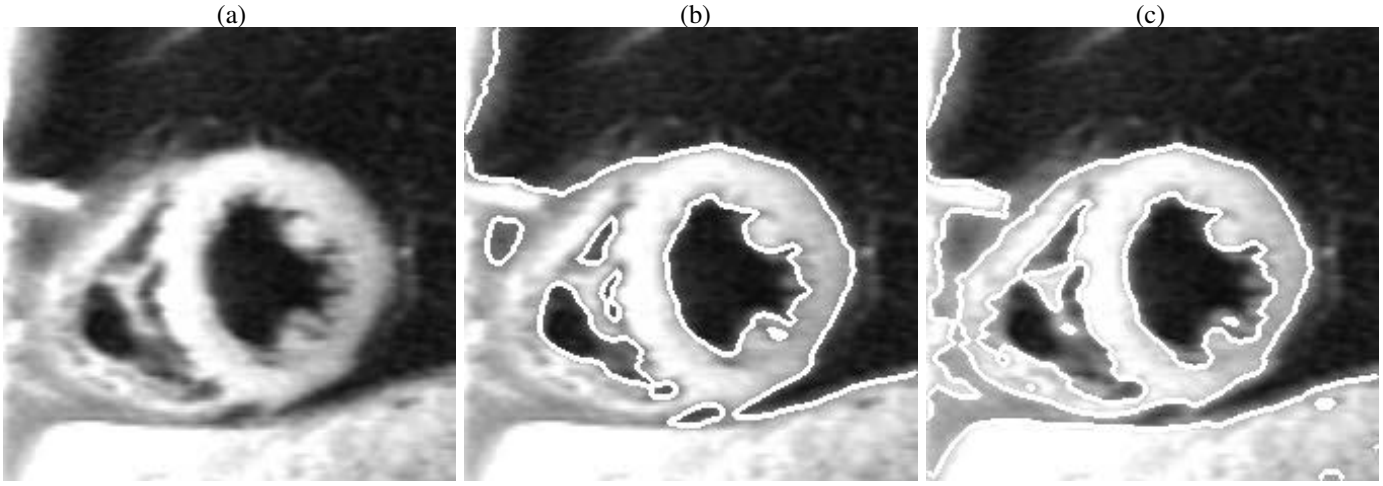

Fig. 4. Cardiac MRI image: (a) the original image and the segmentation results by (b) the MSCV model and (c) the new model.

IV. Numerical Experiments

In this section, we test effectiveness of the new hybrid model incorporating the method of background subtraction (MBS) and the initialization technique presented in Section III. Set $\alpha = \beta = 1$ in the model (1). We choose $m_x = m_y$ for the coarse mesh, to be specified for each example, and $\phi_{\max} = 10^{-4}$ for the initialization (6). For the edge detector defined in (2), set $\zeta = 0.1$ and $p = 1$; $J*$ is defined as a weighted average utilizing pixel values in the 3×3 window.

In Figure 3, we use the same synthetic image in Figure 1 to verify effectiveness of the MBS in the new model. We set $m_x = m_y = 30$ for the coarse mesh in the MBS. As one can see from the figure, the new model detects only the desired edges in two ADI iterations; the new model is efficient and reliable. For this example, the background $\widetilde{u}$ is computed as remarked at the end of Section II, i.e., $\widetilde{u} \geq u^0$.

In Figures 4-6, we will compare performances of the MSCV model and the new model.

Figure 4 presents a cardiac MRI image and segmentation results superposed on it. Set $m_x = m_y = 30$. The original image in Figure 4(a), a capture of a human heart, is a short axis blood-suppressed image at the distal ventricles using the MRI technique. The image reveals noise and unclear edges over the whole image domain. As depicted in Figure 4(b), the MSCV model shows difficulties in the detection of edges, particularly around the lower left corner of the image. The segmentation is obtained to be the best among all possible results from the MSCV model; it has taken 10 ADI iterations. On the other hand, the new model can detect the desired edges successfully as shown in Figure 4(c). Furthermore, the computation is much more efficient due to the initialization technique; the segmentation integration converges just in two ADI iterations.

The image in the above example involves a relatively smooth background and the MBS can produce an essentially binary image (δu), which in turn makes the segmentation algorithm detect desired edges satisfactorily and efficiently. In the following examples, we will deal with medical images having backgrounds that are non-trivial but difficult to subtract either conceptually or computationally.

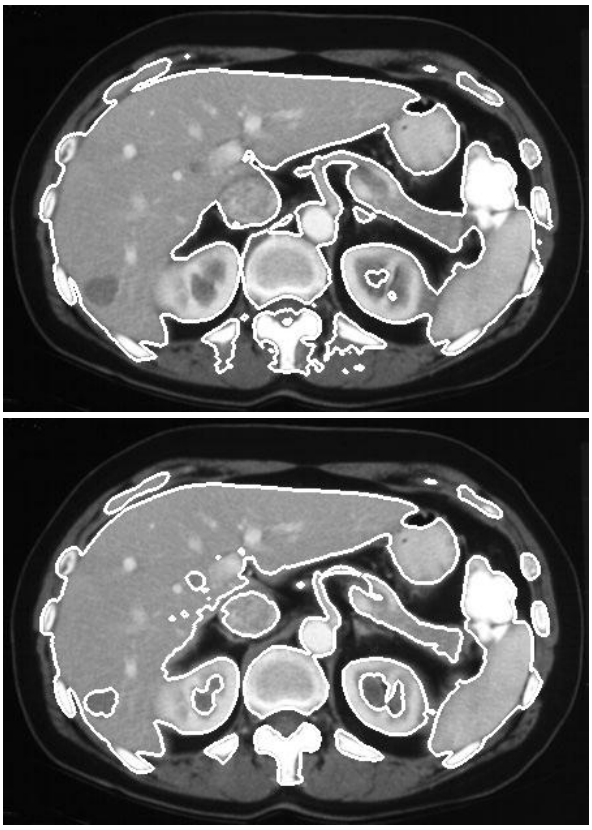

Fig. 5. MRI scan showing possible tumor in the liver: the segmentation results by (top) the MSCV model and (bottom) the new model.

In Figure 5, we select an MRI section of a human liver which shows a possible cancer tumor inside. We do not show the original image, due to a space limit, for this example. As one

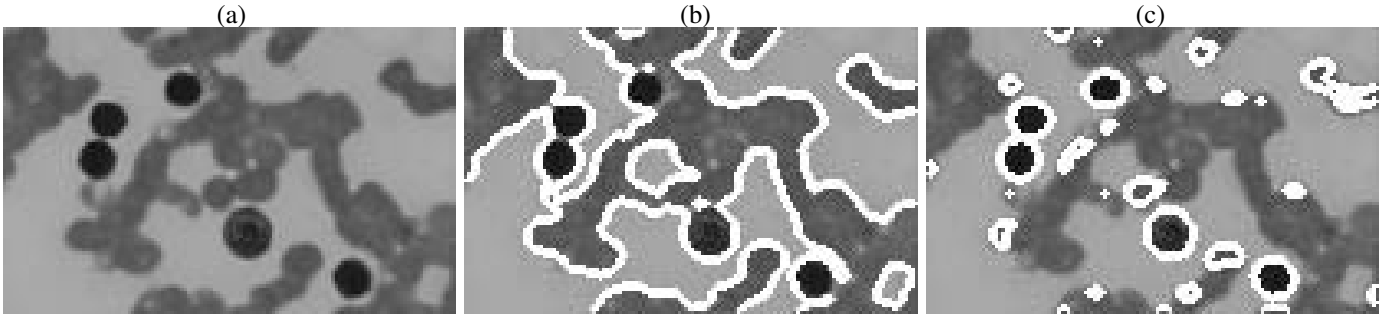

Fig. 6. Leukemia image: (a) the original image and the segmentation results by (b) the MSCV model and (c) the new model.

can see from the top figure, the MSCV model can detect only the (outer) boundary of the liver, which is not satisfactory. On the other hand, our new model (with $m_x = m_y = 40$) can locate every significant spots inside the liver, again in two ADI iterations, as shown in the bottom figure.

Figure 6(a) is an image of acute granulocytic leukemia and red blood cells. Here the darkest particles are the granulocyte cells which cause leukemia and the other particles are the red blood cells. Figure 6(b) shows the segmentation result of the MSCV model, in which the particle edges are formed unclearly and therefore the granulocyte cells cannot be located. On the other hand, our new model can detect the granulocyte cells successfully, as presented in Figure 6(c), although it has also detected a few parts of red blood cells. A post-processing can be applied to remove the undesired particles. For this example, we set $m_x = m_y = 2$.

V. Conclusions

We have considered an efficient and reliable algorithm for PDE-based segmentation. A hybrid model has been suggested combining a gradient-based model and the level set formulation of the Mumford-Shah minimization. We have introduced a linearized alternating direction implicit (ADI) method for an efficient time integration and an initialization technique for a fast evolution of the level set function. The method of background subtraction have been adopted and refined in order to improve reliability of the model. Numerical experiments has shown that our new algorithm can locate the zero-level set (edges) accurately in 2-4 ADI iterations.

References

[1] M. Bichsel, "Analyzing a scene's picture set under varying light," *Computer Vision and Image Understanding*, vol. 71, no. 3, pp. 271–280, 1998.

[2] A. Bieniek and A. Moga, "An efficient watershed algorithm based on connected components," *Pattern Recog.*, vol. 33, no. 6, pp. 907–916, 2000.

[3] T. Chan and L. Vese, "Active contours without edges," *IEEE Trans. Image Process.*, vol. 10, pp. 266–277, 2001.

[4] ——, "A level set algorithm for minimizing the Mumford-Shah functional in image processing," in *IEEE/Comput. Soc. Proc. of the First IEEE Workshop on Variational and Level Set Methods in Computer Vision*, 2001, pp. 161–168.

[5] J. Clark, "Authenticating edges produced by zero-crossing algorithms," *IEEE Trans. Pattern Anal. Machine Intell.*, vol. 12, no. 8, pp. 830–841, 1989.

[6] J. Douglas, Jr. and S. Kim, "Improved accuracy for locally one-dimensional methods for parabolic equations," *Mathematical Models and Methods in Applied Sciences*, vol. 11, pp. 1563–1579, 2001.

[7] J. Douglas, Jr. and H. Rachford, "On the numerical solution of heat conduction problems in two and three space variables," *Transaction of the American Mathematical Society*, vol. 82, pp. 421–439, 1960.

[8] M. Drew, J. Wei, and Z.-N. Li, "Illumination invariant image retrieval and video segmentation," *Pattern Recog.*, vol. 32, no. 8, pp. 1369–1388, 1999.

[9] S. Gunn, "On the discrete representation of the Laplacian of a Gaussian," *Pattern Recog.*, vol. 32, no. 8, pp. 1463–1472, 1999.

[10] J. Haddon and J. Boyce, "Image segmentaion by unifying region and boundary information," *IEEE Trans. Pattern Anal. Machine Intell.*, vol. 12, no. 10, pp. 929–948, 1990.

[11] K. Haris, S. Efstratiadis, N. Maglaveras, and A. Katsaggelos, "Hybeid image segmentation using watersheds and fast region merging," *IEEE Trans. Image Processing*, vol. 7, no. 12, pp. 1684–1699, 1998.

[12] P. Hill, C. Canagarajah, and D. Bull, "Texture gradient based watershed segmentation," in *2002 IEEE International Conference on Acoustics, Speech, and Signal Processing*, vol. 4, Orlando, FL, USA, 2002, pp. 3381–3384.

[13] S. Ji and H. Park, "Image segmentation of color image based on region coherency," in *Proceedings 1998 International Conference on Image Processing*, vol. 1, Chicago, IL, USA, 1998, pp. 80–83.

[14] M. Kass, A. Witkin, and D. Terzopoulos, "Snakes: Acitive contour models," *Int. J. Comput. Vision*, vol. 1, pp. 321–331, 1988.

[15] S. Kim, "A hybrid level set approach for efficient and reliable image segmentation," (To appear in Proceedings of 2005 IEEE ISSPIT).

[16] F. Meyer and S. Beucher, "Morphological segmentation," *J. of Visual Communications ans Image Representation*, vol. 1, pp. 21–46, 1990.

[17] D. Mumford and J. Shah, "Optimal approximation by piecewise smooth functions and associated variational problems," *Comm. Pure Appl. Math.*, vol. 42, pp. 577–685, 1989.

[18] S. Osher and J. Sethian, "Fronts propagating with curvature dependent speed: algorithms based on Hamilton-Jacobi formulations," *J. Comp. Phys.*, vol. 79, pp. 12–49, 1988.

[19] L. Shapiro and G. Stockman, *Computer Vision*. Upper Saddle River, NJ: Prentice Hall, 2001.

[20] H.-K. Zhao, T. Chan, B. Merriman, and S. Osher, "A variational level set approach to multiphase motion," *J. Comput. Phys.*, vol. 127, pp. 179–195, 1996.